<u>HADRONIC FINAL STATES IN MUON INTERACTIONS</u>

H.E. Montgomery

CERN

Geneva

A review is made of experimental data on the final state hadronic system produced in deep inelastic scattering of muons. The data are compared with earlier results from electron scattering experiments and with the relevant theoretical models.

INTRODUCTION

Deep inelastic scattering of muons and electrons on nucleons has provided much detailed information on the distributions of partons (quarks and gluons) in the nucleon [1]. Experimental measurements of the hadronic final states produced in these interactions give complementary information as to the way the transient quark systems evolve into hadrons. Data at the highest energies are also beginning to test the QCD picture of the hard scattering processes involved.

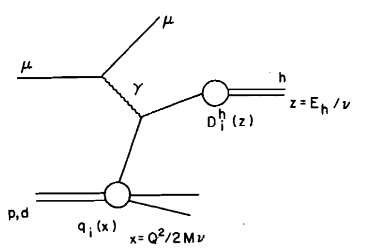

$$\frac{1}{N_\mu}\frac{dN^h}{dz} = \sum_i \epsilon_i(x)/D_i^h(z)$$

$$\epsilon_i = e_i^2\, q_i(x) \qquad i = u,d,s,\bar{u} \;\ldots.$$

$$h = \pi^{\pm,0},\ K^{\pm},\ K^{0},\ \overline{K^{0}} \;\ldots.$$

$$W^2 = 2M\nu - Q^2 + M^2$$

$$x_F \simeq \frac{2p_{\parallel}^{cms}}{W}$$

Fig. 1 - Quark Parton Model diagram of hadron production in muon scattering.

In this paper the experimental data from recent high energy muon scattering experiments will be reviewed within the above context and, where relevant, reference will also be made to earlier electron scattering experiments.

The basic Quark Parton Model (QPM) picture of the process is illustrated in Fig. 1. The virtual photon interacts with a parton, i, whose momentum distribution within the target is $q_i(x)$. The parton then fragments to produce a hadron h, this process is described by the function $D_i^h(z)$. The differential multiplicity $(1/N)(dN/dz)^h(x,z)$ is then given by the incoherent sum of these processes where the sum runs over all quarks and antiquarks in the nucleon. Within the QCD framework this simple picture is modified in two ways. Firstly both the quark distribution functions and fragmentation functions should evolve as a function of Q^2. Secondly there are additional subprocesses, involving either gluons present in the nucleon or the emission of gluons by the interacting quark, which can give corrections to the basic QPM approach.

THE EXPERIMENTS

There have been two recent high energy muon scattering experiments with the capability to detect the produced hadrons.

CHICAGO, HARVARD, ILLINOIS, OXFORD COLLABORATION (CHIO)

The apparatus used in this experiment [2] is sketched in fig. 2(a). It used a 1.5 metre liquid hydrogen or deuterium target in the muon beam at FNAL. The scattered muon and the final state charged hadrons were momentum analysed in the multiparticle spectrometer based on the large apercure Chicago Cyclotron magnet. Limited particle identification was possible in the 18 cell Nitrogen Cerenkov counter downstream of the magnet.

THE EUROPEAN MUON COLLABORATION (EMC)

The EMC experiment at CERN has an experimental layout [3] which is conceptually very similar to that of CHIO. A 6 metre long liquid hydrogen or deuterium target was used during the data taking however the hadron data analysis has so far used only the downstream 2 or 3 metres to avoid large corrections for reinteraction of the hadrons. Again limited identification of the produced hadrons was achieved with a single 78 cell Cerenkov counter [4] which could be filled with either Nitrogen or Neon. In this experiment there was also added a large lead glass wall equipped with a preshower system [5] which permitted measurements of pizero mesons and photons some preliminary results from which will be presented here.

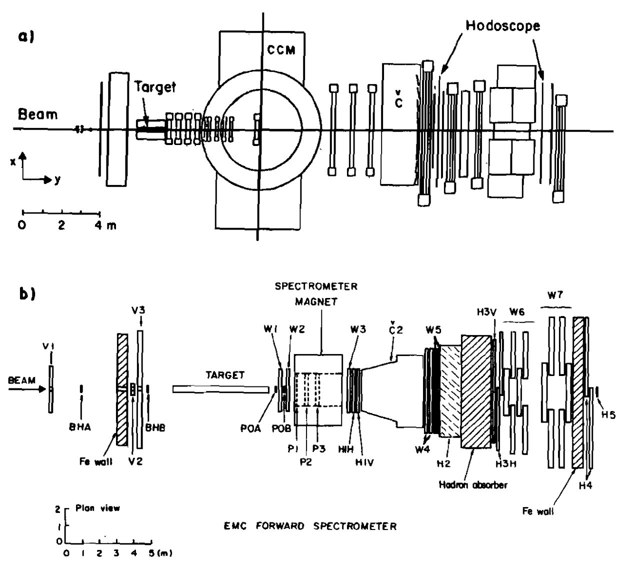

Fig. 2 - a) sketch of CHIO collaboration experiment.
b) sketch of EMC collaboration experiment.

IDENTIFIED MESONS

Elaboration of the basic (QPM) picture of deep inelastic scattering leads to a series of rather well defined predictions. Some of these predictions have been tested at low to moderate values of Q^2 and W^2 and a summary of the situation is given in the reviews of Hand [6] and Seghal [7] at the Hamburg conference in 1977.

A clear prediction of the QPM is

$$\frac{1}{N}\frac{dN^{\pi^0}}{dz} = \frac{1}{2}\left(\frac{1}{N}\frac{dN^{\pi^+}}{dz} + \frac{1}{N}\frac{dN^{\pi^-}}{dz}\right)$$

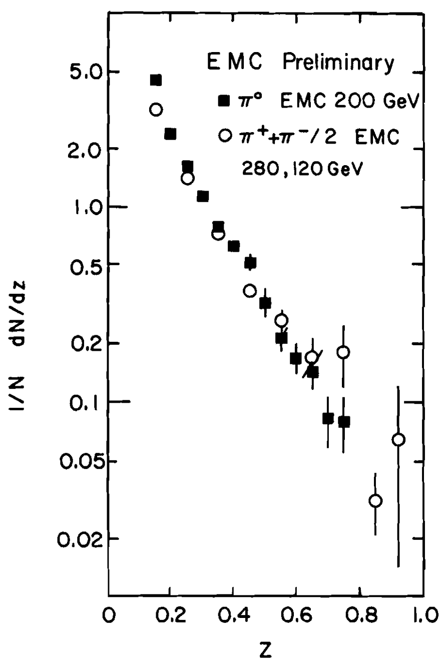

Fig. 3 - Comparison of z distributions of and $\frac{\pi^+ + \pi^-}{2}$ from EMC experiment.

This condition was satisfied at low energies [8] and in fig. 3 data from EMC, in which both charged and neutral pions are identified, indicates no strong departure from the QPM.

The description of kaon production within the QPM is quite complicated. Imposition of isospin invariance and charge conjugation only reduces the number of independent fragmentation functions to 6. Experiments are not however adequate to determine all of these and further assumptions have to be made or models constructed. Assuming $D_{\bar{s}}^{K^+} = D_u^{\pi^+}$ and further that some contributions, from the unfavoured fragmentations of minority quarks, can be ignored then:

$$\frac{1}{N}\frac{dN^{K^+}}{dz} = \epsilon_u D_u^{K^+} + \epsilon_{\bar{u}} D_u^{K^-} + \epsilon_{\bar{s}} D_u^{\pi^+}$$

$$\frac{1}{N}\frac{dN^{K^-}}{dz} = \epsilon_u D_u^{K^-} + \epsilon_{\bar{u}} D_u^{K^+} + \epsilon_s D_u^{\pi^+}$$

giving two unknowns, (ϵ_i assumed known). Sehgal [7] used similar assumptions to determine $D_u^{K^+}$ and $D_u^{K^-}$ and his fits are compared with the data in fig. 4. The EMC data were not available at the time of his fit. A popular model of fragmentation is that of Field and Feynman [FF2,9] who describe kaon production with the probability γ_s to produce an $s\bar{s}$ quark pair at any point in the fragmentation chain. Their original choice was $\gamma_s = 0.2$ and curves based [10] on this choice lie systematically higher than the data in fig. 4.

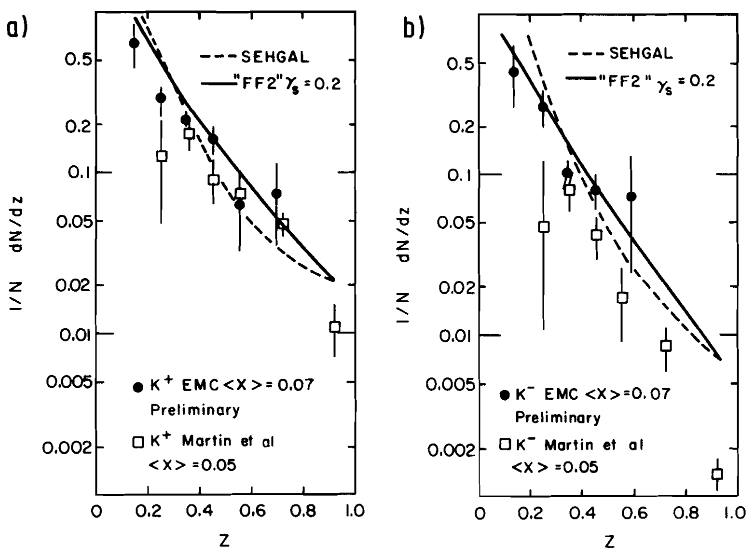

Fig. 4 - a) z distribution of K^+ mesons
b) z distribution of K^- mesons
See text for discussion of curves

Neutral kaon measurements from the DECO experiment [11] and CHIO [12] are shown in fig. 5 and compared with some neutrino measurements [13,14], that there is some measure of agreement fits with the expectation that u quark fragmentation is important in all cases. Again the data lie below the expectations based on γ_s = 0.2. However, the relative kaon yield with respect to pions is also very sensitive to the fraction of vector mesons produced, since the strange vector mesons decay also to pions, and this fraction is not well known.

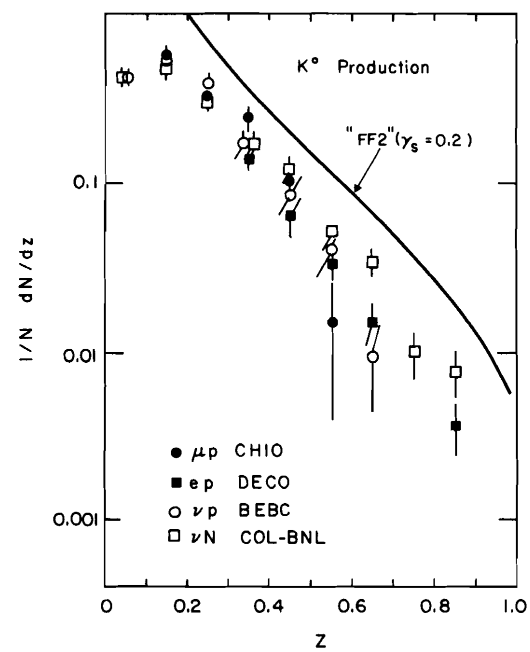

Fig. 5 - K° production compared with "FF2" prediction for γ_s = 0.2.

CHIO [15] have compared, fig. 6, their K/π ratio with e^+e^- data at a similar cms energy and find qualitative agreement which they attribute to the dominance of production from the sea quarks at their low value of x. Their ratios K^+/π^+ and K^-/π^- are displayed as a function of p_T in fig. 7. A systematic increase is observed which can be attributed to the stronger contribution of resonance decay to the pion yield.

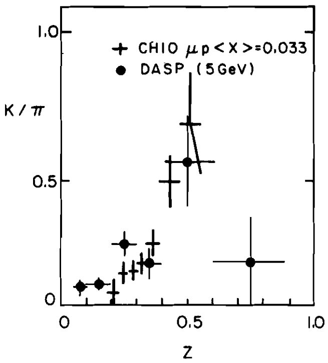

Fig. 6 - Comparison of K/π ratio as a function of z between CHIO experiment and e^+e^- at a similar centre of mass energy.

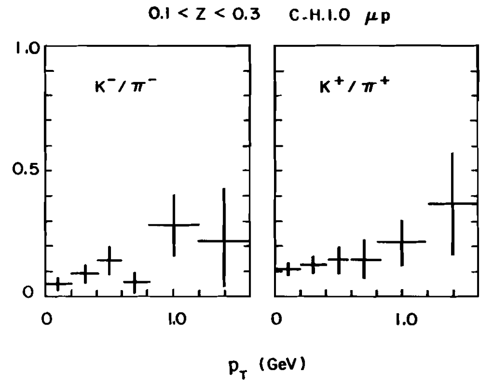

Fig. 7 - K/π ratio as a function of p_T.

It should be noted that none of the conclusions of this section are very quantitative. This is due to the limited nature of the experimental data available. There is, given a single Cerenkov counter, a strong correlation between the kinematic variables of the hadron (z, $P_T{}^2$) and of the muon (Q^2,x) for which identification can be made. Especially in the case of charged kaons, assumptions have to be made about x and/or Q^2 independence which are not true in general.

BARYON PRODUCTION

Proton production in low energy electroproduction was the subject of considerable experimental investigation [16,17,18,19], due in considerable part to the suggestion [20] that events with a forward going proton should contribute a large fraction to the total cross section. The observed x_F distribution peaks at $x_F \sim -0.2$ and falls rather steeply for x_F

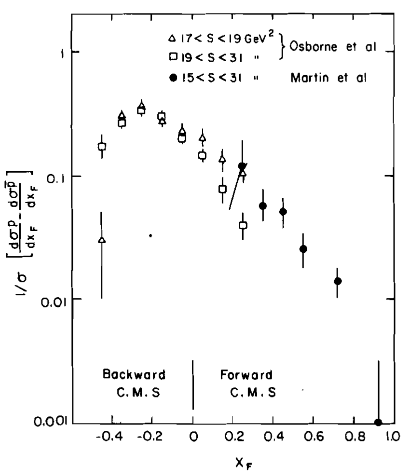

Fig 8 - Feynman x distribution of protons from electroproduction experiments at SLAC.

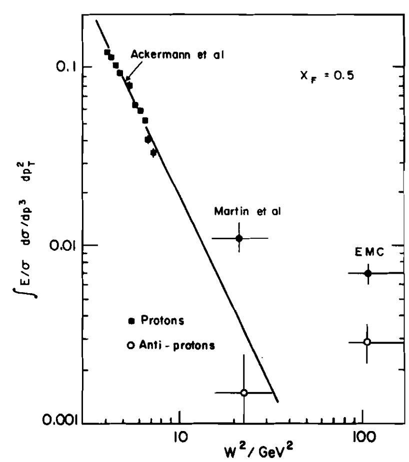

Fig. 9 - W dependence of proton production for fixed $x_F = 0.5$.

positive as illustrated in fig. 8. Furthermore, the yield for $x_F > 0$ decreases strongly with W, as shown in fig. 9, for W < 4.5 GeV, suggesting that the protons are basically target fragments which can at low energy spill into the forward direction. In addition to the low energy points, fig. 9 contains a point taken from a recent measurement [21] of proton production at high energies which does not follow the low energy trend and, given the antiproton measurement as well, suggests that a new mechanism may be contributing.

The z distributions observed in these data are shown in fig. 10(a) and the antiproton yield is seen to be close to that of the protons at low z but to fall more steeply. Similar behaviour [22] was observed for identified hadrons and when the ratio is made to the total hadron yields the results shown in fig. 10(b) are obtained. The point made earlier about hidden correlation between hadron and muon variable is also valid here [23].

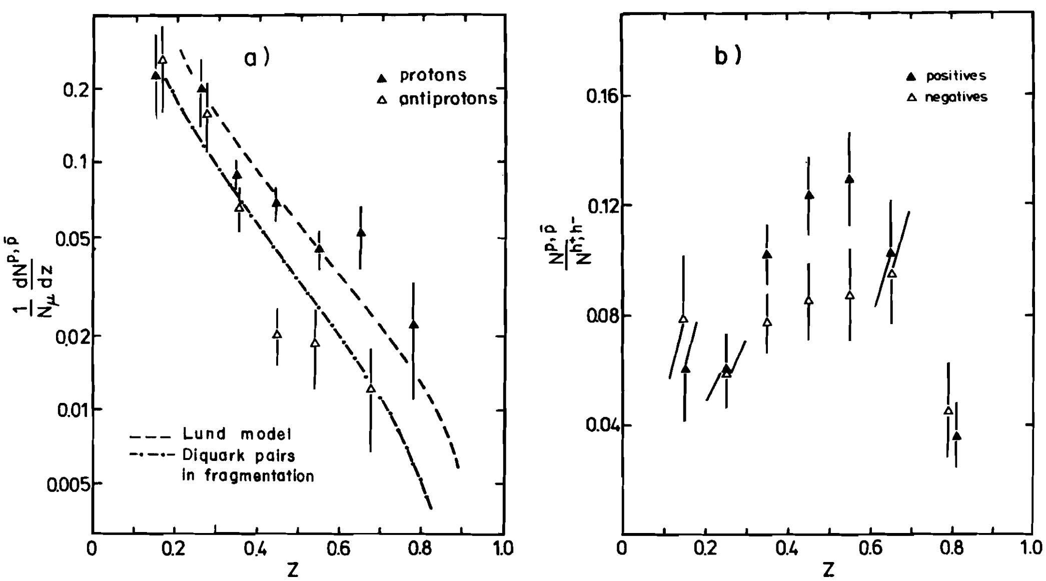

Fig. 10 - a) z distributions of protons and antiprotons from the EMC experiment. Curves are predictions of the LUND model

b) Ratio as a function of z of protons (antiprotons) to all hadrons of the same sign.

For $0.4 < z < 0.6$ a wide range of Q^2 and x is available and no Q^2 dependence is observed at fixed x. In particular no decrease with Q^2 is observed which discourages the possibility that the photon scattering from diquarks in the nucleon [24,25] could be the main source of these protons . Integrated over Q^2, the x dependence, for this same z range, is displayed in fig. 11(a) and a rise of the protons with x is observed while the antiprotons are constant or fall slightly. Again taking the ratio to all hadrons of the same charge, fig. 11(b), removes most of these tendencies. The suggestion from the data is therefore that the protons do not behave specially and could well be produced in a similar quark fragmentation process. The p_T distribution, fig. 12, is also quite similar to that for all hadrons.

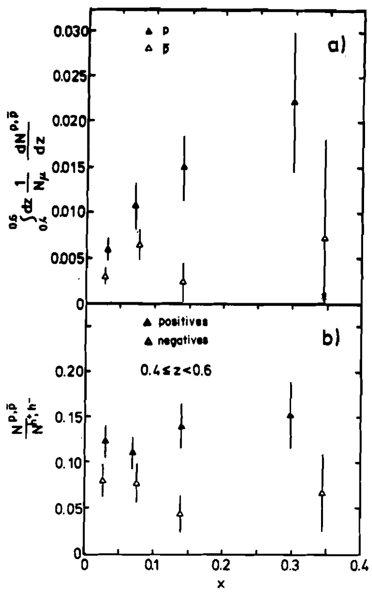

Fig. 11 - a) x dependence of p ($\bar{p}$) production for 0.4 < z < 0.6 from EMC.
b) corresponding ratio with all hadrons of the same sign

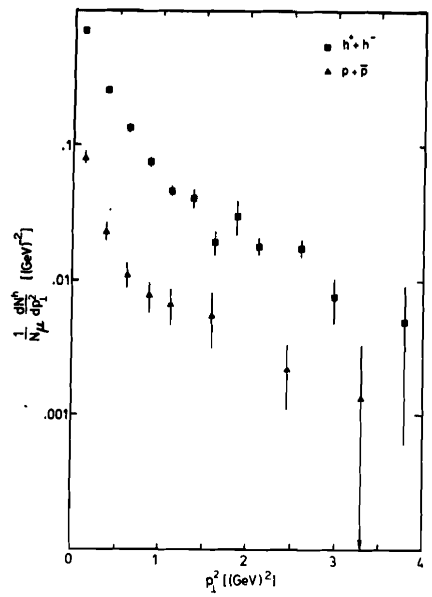

Fig. 12 - p_T dependence of proton+antiproton production compared with that for all hadrons in the same kinematic range.

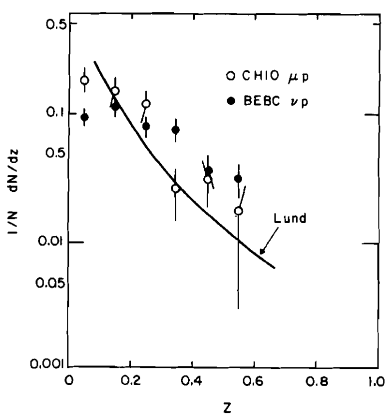

Fig. 13 - Comparison of data on Λ production compared with predictions of LUND model.

Recently a model [26] incorporating diquark-antidiquark pairs in the fragmentation process, has been proposed to explain the baryon production observed in e^+e^- experiments. The expected yields within this model [27] are compared to the data in fig. 10 and good agreement is achieved. The comparison of the same model with the available data [11,12,13,14] for Λ production shown in fig. 13 is not however as impressive. The model has the nice features that it is rather specific about its production mechanisms and the NA9 [28] stage of the EMC experiment at CERN with its rather extensive particle identification should critically test these.

SCALE BREAKING, FACTORISATION BREAKING

In the previous two sections it was often assumed that the basic QPM attributes, scaling and factorisation (the product structure of (1/N)(dN/dz)), were valid. Violations of scaling can arise due to the leading order QCD evolution of the fragmentation functions [29] which imply

$$D(z) \to D(z,Q^2).$$

The factorization structure is maintained at this order. In next to leading order the introduction of extra graphs leads to non factorization [30,31] and in principle a further modification of the Q^2 evolution should be expected [32].

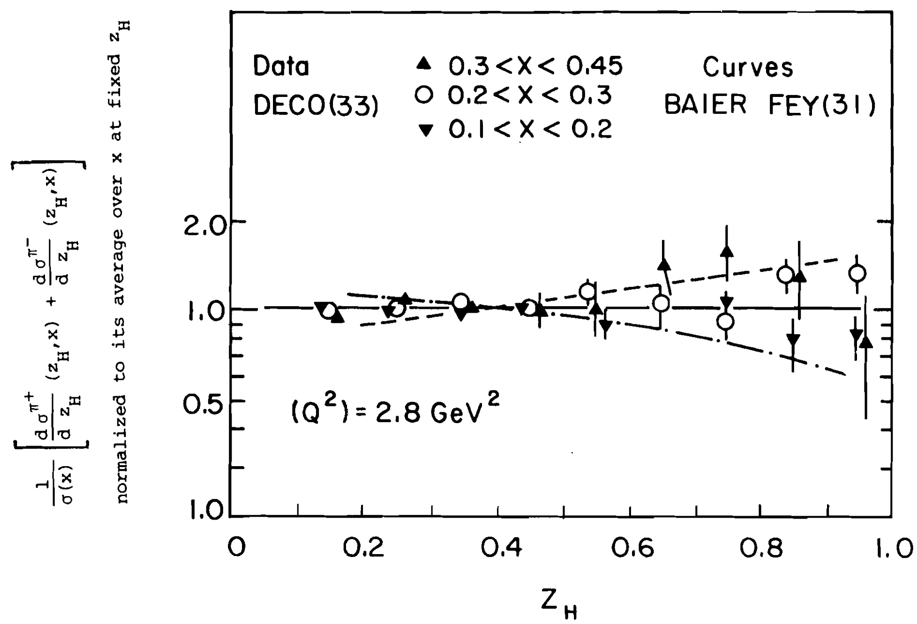

Fig. 14 - Comparison of data from the DECO electroproduction experiment with the expectations of next to leading order QCD.

Data from the DECO experiment [33] are shown in fig. 14, they were presented by the experimenters as support, within errors, for factorisation. The curves from Baier and Fey [31] however suggest that the trends in the data are consistent with QCD expectations.

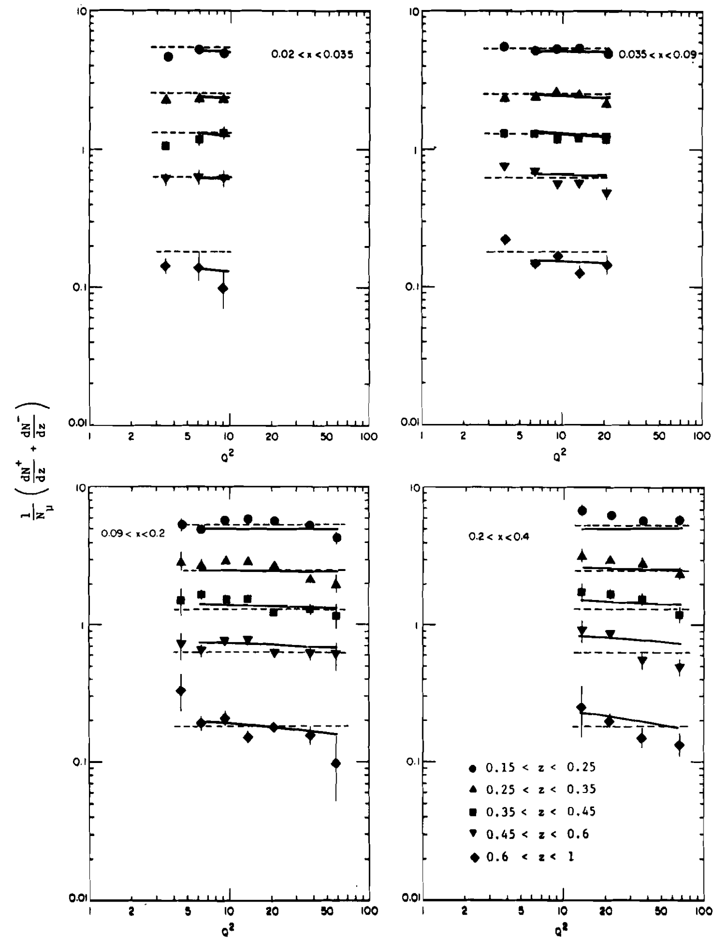

Fig. 15 - EMC data at different fixed z values in a different x regions as a function of Q^2. The dotted (-----) curve is from a QPM calculation the solid line from the QCD calculation of Baier and Fey.

New preliminary data from EMC are based on ∿ 50000 events at 120 and 280 GeV with a minimum W^2 of 15 GeV^2. Since the study requires the highest statistics over a wide range of x and Q^2 these data contain all charged hadrons, unidentified. The basic data consist of a total of 19 z distributions with different Q^2 and/or x values. These data are plotted versus Q^2 for each z value and four different x values in fig. 15. The data show a weak but systematic

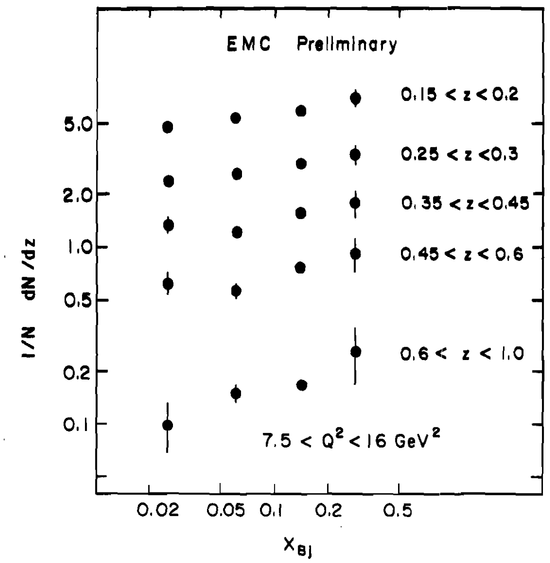

Fig. 16 - EMC data in a narrow Q^2 range as a function of Bjorken x.

decrease with increasing Q^2. This behaviour which tends to be strongest at higher z is not at all reproduced by the QPM. The calculation of Baier and Fey [31] has been used to estimate the expected next to leading order QCD behaviour. The trends of the data are indeed reproduced however given the large number of input functions to this calculation and the theoretical caveats [32] no quantitative comparison has yet been attempted.

The x dependence for the range $7.5 < Q^2 < 16$ GeV^2 is shown in fig. 16 and it is clear that an x dependence (non-factorisation) is observed. The complete data set is displayed in this projection in fig. 17 and again, for comparison, the QPM and QCD curves. It is then seen that also the x dependence is reproduced by the QCD based calculation. What is now required is a phenomenological analysis to match these data and extract the relevant parameters.

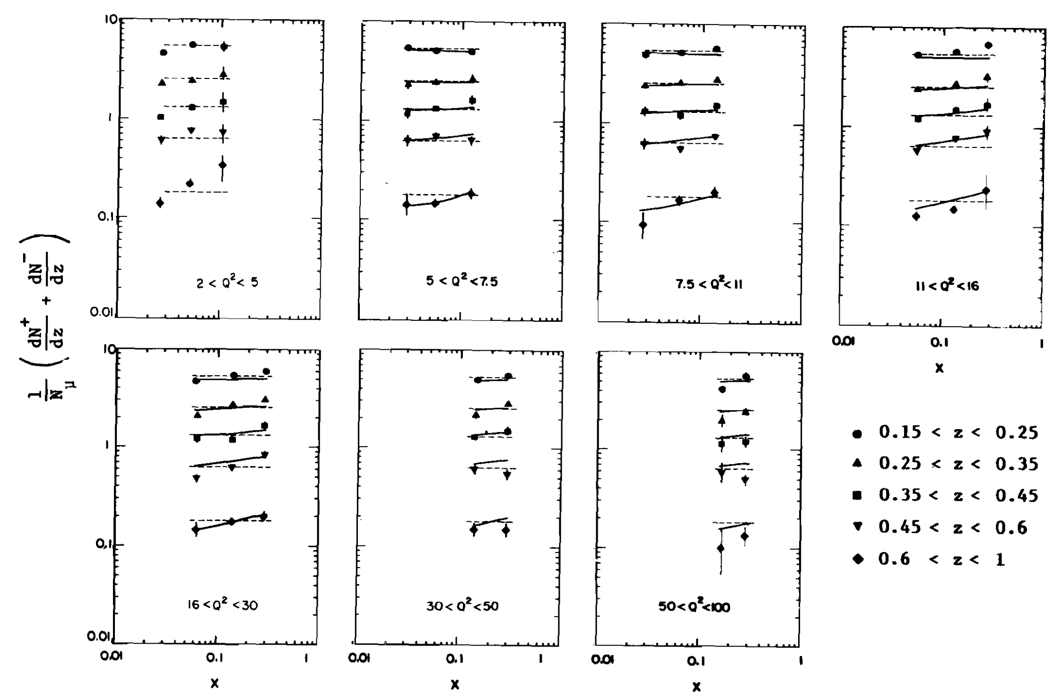

Fig. 17 - As for fig. 16 but for 7 different Q^2 ranges. Curves as for fig. 15.

p_T DISTRIBUTION, EVENT STRUCTURES

The same next to leading order QCD graphs which are responsible for the effects described in the previous section, can, especially by hard gluon emission lead to a general broadening of hadron p_T distributions with increasing W^2 and eventually to the production of separated jets from the different partons. In deep inelastic scattering there are also two non-perturbative sources of p_T. First, the partons will have an internal transverse momentum k_T within the nucleon, second, in the fragmentation of the quark to the observable hadrons the hadrons acquire a $p_{T\,frag}$.

The dependence of $\langle p_T^2 \rangle$ on z, Q^2 and W^2 has been studied by CHIO [34] and by EMC [35]. The experimental data from EMC, fig. 18, including preliminary results from 120 GeV charged particle and 200 GeV π^0 data give a rather complete picture of the rise with W^2 which is interpreted as being due to perturbative QCD [36,37,38]. These data [35] however also required a rather large value $\langle k_T^2 \rangle \sim 0.6$ GeV^2 to describe the z dependence of $\langle p_T^2 \rangle$.

EMC have also presented data [39] which show some evidence for jet structure at 280 GeV. There are now preliminary results available from the 120 GeV data which extend to lower W. Only events with $N_{had} \geq 4$ are considered, the (well measured) virtual photon direction is defined as the event axis and the plane of the event is found which contains this axis and which minimises the p_T^2 of the hadrons perpendicular to this plane. An angle ψ about the normal to this plane, fig. 19, may then be defined and the event ordered such that the highest p_T particle has $\psi < 0$. The Σp_T^2 "in" and "out" of this plane for the two data samples are shown together in fig. 20. Since the effective z cut

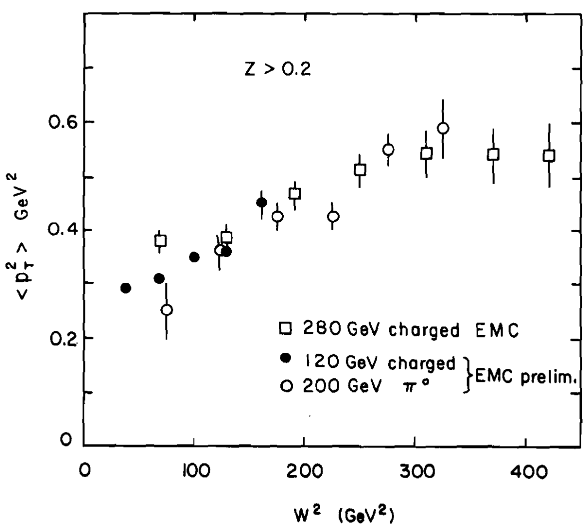

Fig. 18 - Mean p_T^2 values as a function of W^2 for three different EMC measurements.

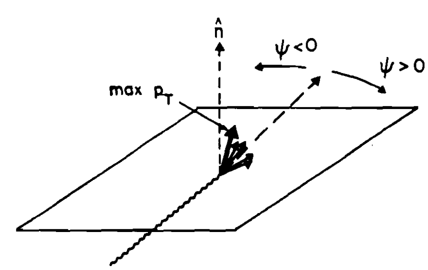

Fig. 19 - Diagram showing definition of event plane and the angle ψ used in the jet analyses.

for these two data samples is very similar, the Monte Carlo model [40] predicts very little change from one energy to the other in the absence of QCD. The data are well described by these QPM curves out to $\Sigma p_{T\,in}^2 \sim 2$ GeV², but beyond this there is a tail in each data set which is however much more significant at 280 GeV. These tails and their change with energy are qualitatively reproduced by the QCD model. The difficulty to describe these data with modified fragmentation models is illustrated in fig. 21 where the 280 GeV data are compared with the conventional QPM with σ_q = 310 MeV and also with σ_q = 470 MeV. In the latter case a tail is produced but which looks nothing like the data.

The energy flow $\int z\,(dN/dz d\psi)\,dz$ as a function of the angle ψ is shown in fig. 22(a) and a strong collimation about $\psi = 0$ is observed. When a requirement $p_{T\,max}^2 > 2$ GeV² is imposed on the events a two lobe structure appears (fig. 22(b)). In principle such a structure can result from momentum conservation but the failure of the σ_q = 470 MeV Monte-Carlo to produce the observed shape should be contrasted with the qualitative agreement of the curve produced by the QCD Monte-Carlo.

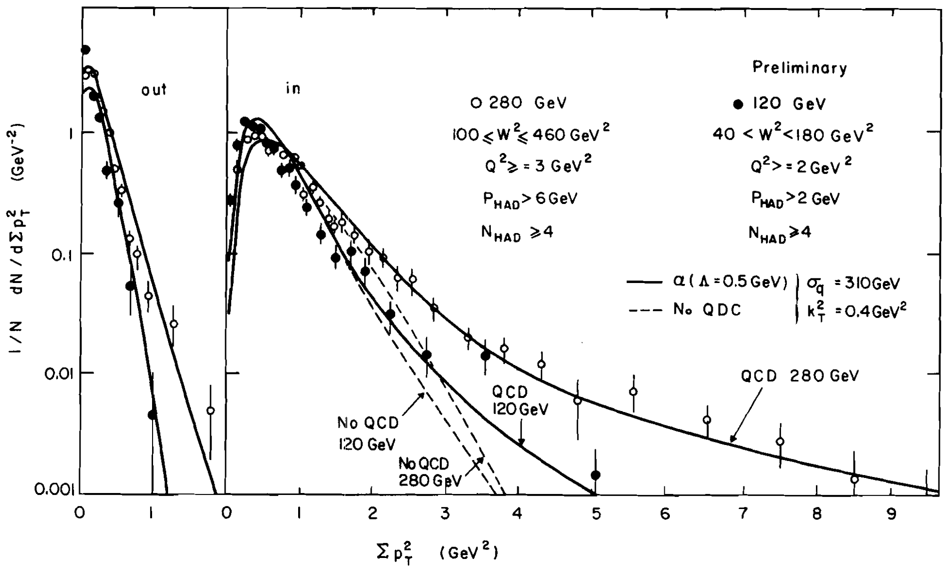

Fig. 20 – Σp_T^2 in and out of the event plane for two data samples with much different W ranges. Curves are from the LUND Monte Carlo Model.

The momentum flow in the plane perpendicular to both the event axis and the event plane (p_T flow) is shown in fig. 23 as a function of azimuth (ϕ) about the event axis. The $\phi = 0$ is defined by the $p_{T\,max}$ particle which is then <u>not</u> included in the plot. When no cut is applied the data show the "away" side correlation resulting from momentum conservation but no other feature. When a $p_{T\,max}^2 > 2$ GeV² cut is applied the away side correlation is enhanced and moreover a near side enhancement appears. Such a structure is well produced by the QCD model but could in principle be also due to resonance production and decay. That this is unlikely is shown by the σ_q = 470 MeV curve which, although containing resonances in the conventional vector meson/pseudoscalar meson = 1 proportion, has no significant enhancement.

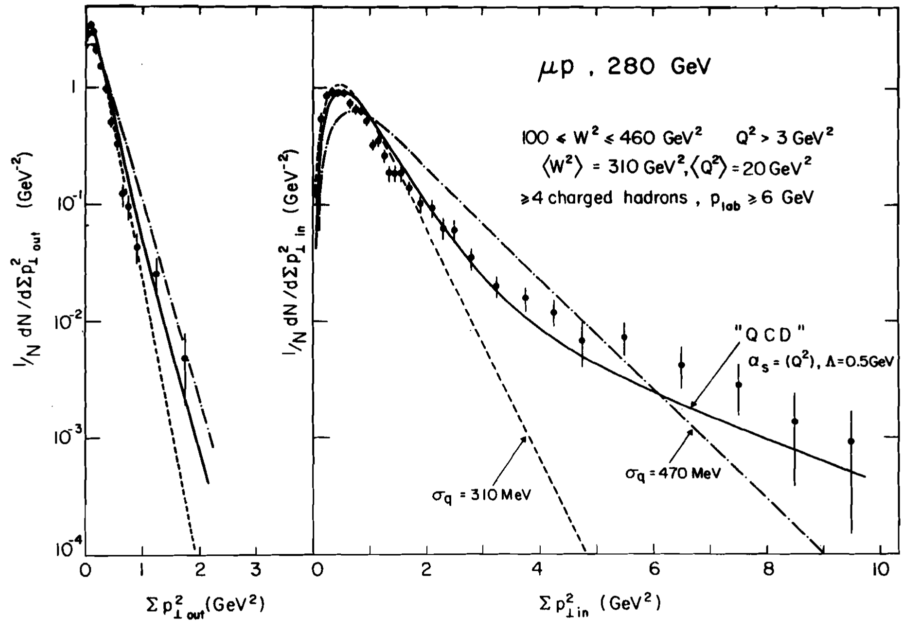

Fig. 21 - Comparison of the 280 GeV muon scattering data with the QCD model and with conventional fragmentation with two different fragmentation p_T (σ_q) values.

As mentioned earlier a potential and apparently significant source of hadron p_T is the fermi momentum of the parton. Within the models the vector sum $(\vec{\Sigma}p_T)^2$ of the produced hadrons is very sensitive to k_T (if all the fragments of the stuck quark could be isolated and measured then $(\vec{\Sigma}p_T)^2$ would be directly $k_T{}^2$). Fig. 24 shows the distribution of $(\vec{\Sigma}p_T)^2$ for those events where greater than 70% of the quark momentum has been observed. The curve is the model using $k_T{}^2 = 0.4$ GeV² and agreement is quite good. The rather large value of $k_T{}^2$ obtained in each of these determinations coupled with the apparent inconsistency suggests that there is a basic lack in the model. This lack may well have been recently resolved since a contribution to this conference [41] suggests that extra soft gluon emission plays a rôle and a residual $\langle k_T{}^2\rangle = (0.4 \text{ GeV})^2$ is deduced after these effects have been taken into account. It should be noted that the experimental data drove the theory in this case.

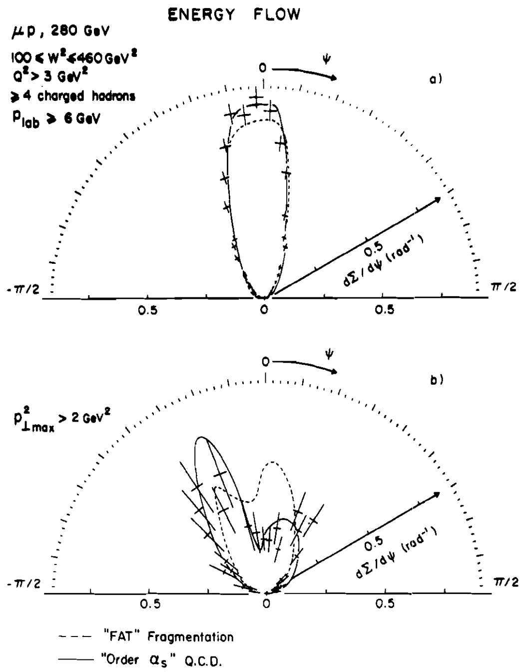

Fig. 22 - Energy flow in the plane of the event, data from EMC, a) with no cuts, b) with requirements that at least one hadron has $p_T{}^2 > 2$ GeV². Solid curve is QCD expectation, the dotted is that of non QCD fragmentation with increased fragmentation p_T.

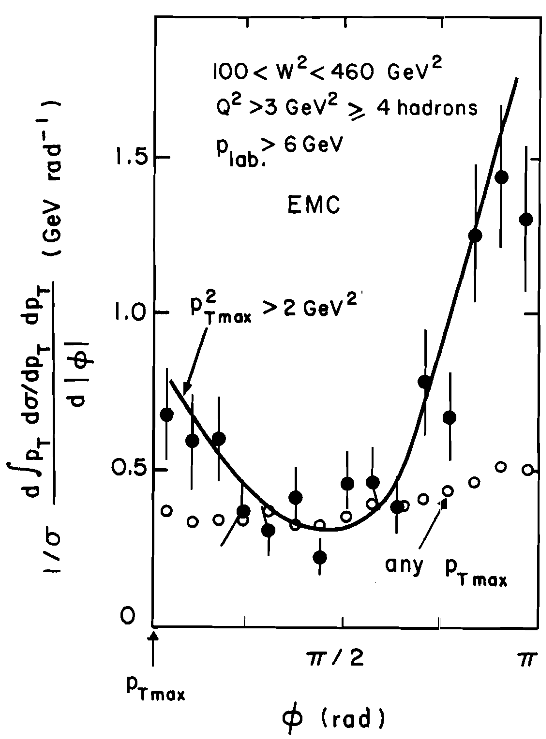

Fig. 23 - Momentum flow in plane perpendicular to the virtual photon. o with no cuts, ● with requirement $P_{T\,max}^{\,2} > 2$ GeV². The particle with the max. $P_T{}^2$ is at the $\phi = 0$. Curve is QCD prediction.

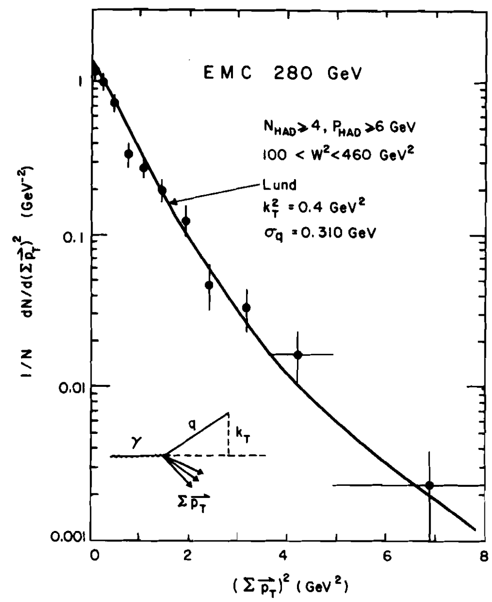

Fig. 24 - Distribution of $(\vec{\Sigma}p_T)^2$ for muoproduction events compared with $k_T^2 = 0.4$ GeV^2.

SUMMARY

A considerable body of experimental data has emerged on deep inelastic hadron production over the last few years. The points covered in this review were as follows.

(a) The QPM can still provide an adequate description of the data on identified meson production however, the traditional $\gamma_s = 0.2$ of Field and Feynman appears to be too high. The data on kaon production are still however too sparse to exclude surprises.

(b) Proton production appears to play a very significant rôle and present data appear to suggest that diquark pair production in the fragmentation process could be the appropriate mechanism. Again improvement in the data can be foreseen which should critically test these models.

(c) Scale breaking and factorisation breaking have been experimentally observed and much phenomenological work is needed to establish whether these can be quantitatively described by next to leading order QCD.

(d) Jet like structures are observed in the data which depart from simple QPM behaviour especially at high W. These structures are consistent with QCD models and alternative explanations would require gross modification of conventional fragmentation models.

Fours years ago in Hamburg, Hand's talk contained a lot of questions to which he expected muon scattering data to provide the answers. It is gratifying to see that indeed most of his questions have been answered and that even more the data obtained have pushed the theorists into a program of modifications to the QPM ideas which were adequate for so long.

I would like to express my thanks to my colleagues in EMC both for the work which contributed to much of the data presented in this talk and for the many discussions which have formed what understanding I have of the subject. The production of this report was only possible due to the excellent work on text and figures by Ariella Mazzari and Claude Rigoni.

REFERENCES

[1] G. Smadja, J. Drees. Review talks presented at this conference.

[2] W.A. Loomis et al., Phys. Rev. D19 (1979) 2543.

[3] E.M.C. O.C. Allkofer et al., Nucl. Instr. & Meth. 179 (1981) 445.

[4] Y. Declais et al., Nucl. Instr. & Meth. 180 (1981) 53.

[5] R. Clifft et al., Nucl. Instr. and Meth. 157 (1978)47.

[6] L.N. Hand. Rapporteurs talk. International Symposium on Lepton and Photon Physics at High-Energies. Ed. F. Guttbrod, Hamburg, 1977.

[7] L.M. Sehgal. Rapporteurs talk. International Symposium on Lepton and Photon at High-Energies. Ed. F. Guttbrod, Hamburg, 1977

[8] Ch. Berger et al., Phys. Lett. 70B (1977) 471.

[9] R.D. Field and R.P. Feynman, Nucl. Phys. B136 (1978) 1

[10] The "FF2" curves were calculated using a program based on a representation of the analytic approximation of Ref. [9] given by J.A. Hassan, Manchester University Preprint, M/C TH 80/31 (1980).

[11] I. Cohen et al., Phys. Rev. Lett. 40 (1978) 1614.

[12] R.G. Hicks et al., Phys. Rev. Lett. 45 (1980) 765.

[13] A.M. Cnops et al., Reported by R.B. Palmer. Proceedings XIIIe Rencontre de Moriond, Les Arcs, 1978, Vol. 2, 361.

[14] H. Grässler et al., CERN-EP/81-56.

[15] J. Proudfoot et al., Submitted to Phys. Rev. Lett. 1981.

[16] A. Sofair et al., Nucl. Phys. B42 (1971) 369.
J.C. Alder et al., Nucl. Phys. B (1972)
E. Lazarus et al., Phys. Rev. Lett. 29 (1972) 1409.
L. Ahrens et al., Phys. Rev. D9 (1974) 1894.
C.J. Bebek et al., Phys. Rev. Lett. 32 (1974) 27.
C.J. Bebek et al., Phys. Rev. Lett. 34 (1975) 1115.
C.J. Bebek et al.. Phys. Rev. D15 (1977) 3077.

[17] H. Ackermann et al., Nucl. Phys. B120 (1977).

[18] L.S. Osborne et al., Phys. Rev. Lett. 41 (1978) 76.

[19] J.F. Martin et al., Phys. Rev. D20 (1979) 5.

[20] S.D. Drell and T.M. Yan, Phys. Rev. Lett. 24 (1970) 855.

[21] E.M.C. J.J. Aubert et al., Phys. Lett. 103B (1981) 388.

[22] E.M.C. J.J. Aubert et al., CERN-EP/80-130 (unpublished).

[23] The correlation between the z range for which protons can be identified and the x defined by the muon scatter means that at low z in fig. 10 a) <x> = 0.05 and at high z, <x> = 0.2. Since the ratio in fig. 10 b) is to be assigned to the <x> of all hadrons, the correlation is different and the high z points are at lower <x> than those in fig. 10 a).

[24] R. Blankenbecler, SLAC-PUB-2512 (1980).

[25] A. Donnachie and P.V. Landshoff, Phys. Lett. 95B (1980) 437.

[26] B. Anderson, G. Gustafson, G. Ingelman and T. Sjöstrand, Lund University Preprint, LU-TP 81-3 (1981).

[27] B. Anderson, G. Gustafson, G. Ingelman and T. Sjöstrand, Lund University Preprint, LU-TP 81-6 (1981).

[28] EMC, CERN/SPSC/80-80 - SPSC/M245 September 1980.

[29] J.F. Owens, Phys. Lett. 76B (1978) 85,
T. Uematsu, Phys. Lett. 79B (1978) 97.

[30] G. Altarelli, R.K. Ellis, G. Martinelli and So-Young Pi, Nucl. Phys. B160 (1979)301.

[31] R. Baier and K. Fey, Z. Physik C, Particles and Fields 2 (1979) 339.

[32] W. Furmanski and R. Petronzio, TH-3046-CERN (1981).

[33] C. Drews et al., Phys. Rev. Lett. 41 (1978)1433.

[34] C. Tao et al, Phys. Rev. Lett. 44 (1980) 1726.

[35] E.M.C., J.J. Aubert et al., Phys. Lett. 95B (1980) 306.

[36] G. Altarelli and G. Martinelli, Phys. Lett. 76B (1978) 89.

[37] B. Andersson, G. Gustafson, G. Ingelman and T. Sjöstrand, Lund University Preprint LU-TP 80-6 (1980).

[38] M. Dechantsreiter, F. Halzen and D.M. Scott, DOW-ER/00881-157 (1980).

[39] EMC, J.J. Aubert et al., Phys. Lett. 100B (1980) 433.

[40] G. Ingelman and T. Sjöstrand, Lund University Preprint, LU-TP 80-12 (1980).

[41] B. Andersson, G. Gustafson, G. Ingelman and T. Sjöstrand, Transverse Momentum Effects of Soft Gluons in Leptoproduction, Paper contributed to this conference.

Discussion

G. Wolf, DESY: You have compared your data for $\mu p \to \mu h^{\pm} X$ with QCD assuming $\Lambda = 0.5$ GeV and you found good agreement. The inclusive data $\mu p \to \mu X$ however yielded $\Lambda \sim 0.1 - 0.2$ GeV. Could the QCD-model fit the $\mu p \to \mu h^{\pm} X$ data also with $\Lambda = 0.1$ or 0.2 GeV?

H. Montgomery: The problem in extracting a value of Λ from these data is that while the height of the $(p_T^2)_{in}$-curve at high p_T^2 is directly proportional to α_s, it is also sensitive to the gluon distribution. I think we have to do a lot more work about the details of quark distribution functions which enter into the generation of the jets. It is not just a question of α_s which enters in here. With a different set of input structure functions and the same value of Λ we get different curves. They are substantially in agreement, but it is a big step to extract in detail a value of Λ.

D. Nachtmann, Univ. Heidelberg: I would like to point out that there is an old sum rule due to Feynman saying that the average number of baryons minus antibaryons in a quark jet should be 1/3, i.e. different from zero. Therefore, you should expect to see baryons and antibaryons in the current fragmentation region. Can you give any number for Feynman's sum rule?

H. Montgomery: If one simply integrates the z-distribution shown from $z = 0.1$ to $z = 1$ one arrives at ~ 0.08 for the protons and 0.06 for the antiprotons. The difference would have a large error but seems to be significantly less than 1/3. We cannot guarantee however that we have all the quark fragments nor do we have all baryons.

B. Esposito, CERN: Did you study the distribution of $\langle p_T^2 \rangle_{in}$ and $\langle p_T^2 \rangle_{out}$ for different W^2?

H. Montgomery: No.

B. Esposito: So you don't know if there is an energy-dependence of the p_T^2 ?

H. Montgomery: We don't have the average values but the $\sum (p_T^2)$ out of the plane is shown in fig. 20.

B. Esposito: But this is $\sum p_T^2$.

H. Montgomery: That's right.

B. Esposito: I asked, if you have the same for the $\langle p_T^2 \rangle_{in/out}$?

H. Montgomery: I said no.

B. Esposito: You know, the difference can come also from the rise of the multiplicity in this variable.

H. Montgomery: Yes. Technically the $<p_T^2>_{in/out}$ is quite hard for us to work with. When you take $<p_T^2>$, then you are dependent on the z-cut. When we make a fixed cut in z and nevertheless try to get a large multiplicity, then for very high W the z-cut pushes us to high hadron-momenta and the data go to zero. We find it very difficult to come out with $<p_T^2>_{in/out}$ - distributions as a function of W^2.